



# Optimizing the soil conservation service curve number model by accounting for rainfall characteristics: a case study of surface water sources in Beijing

Wenlong Song · Jian Jiao · Pengfei Du · Hongjie Liu

Received: 5 May 2020 / Accepted: 7 January 2021 / Published online: 8 February 2021  
© The Author(s), under exclusive licence to Springer Nature Switzerland AG part of Springer Nature 2021

**Abstract** The upper catchment of the Miyun reservoir is an important drinking water source in Beijing. In recent years, researchers have used the soil conservation service curve number (SCS-CN) model to calculate surface runoff for the district. Although the runoff forecasting accuracy was unsatisfactory, the lack of understanding of rainfall processes and their influence on runoff may explain the observed deviations. Our study sought to optimize and assess the SCS-CN model simulation accuracy for the district by proposing an SCS-CN calculation method for each runoff event ( $CN_t$ ) based on observation data for 253 rainfall and runoff events from 7 plots in the Miyun Shixia watershed. This study elucidated a significant positive correlation between the ratio of  $CN_t$  and the average SCS-CN ( $CN_1$ ), as well as the ratio of the maximum  $X$ -minute rainfall amount ( $P_X$ ) to the total rainfall amount for each rainfall event ( $P$ ). Furthermore, a calculation method involving power function equations between  $CN_t/CN_1$  and  $P_X/P$  was proposed for  $CN_t$ . When  $X = 5$  min and

the initial abstraction ratio ( $\lambda$ ) = 0.01, the simulation performance of the optimized model was the highest, with a Nash-Sutcliffe efficiency coefficient of 0.791, which was significantly higher than that of the non-optimized SCS-CN model. The simulation performance for bare and cultivated land was higher than that of other land uses, with  $E_f$  values of 0.831 and 0.828, respectively. Future research should focus on improving the prediction accuracy of runoff events resulting from high-intensity and short-duration rainfall events.

**Keywords** Surface runoff · Soil conservation service curve number · Model improvement · Land use · Miyun

## Introduction

Water balance is the basis for the analysis of hydrological phenomena and hydrological processes. Accurate prediction of surface runoff is crucial for the simulation of hydrological processes, sediment yields, and pollutant fate and transport. Currently, mechanistic and empirical models have been developed to simulate surface runoff. In particular, mechanistic models typically employ calculation methods such as the Green-Ampt infiltration curve (Viji et al. 2015), Philip infiltration curve (Wang et al. 2016), and Horton infiltration curve (Fadadu et al. 2018), among others. However, these methods involve many parameters that are difficult to obtain, which limits their implementation. In contrast, empirical models are relatively simple and require less data input, which makes them more suitable for runoff estimation for the

---

W. Song · J. Jiao · P. Du · H. Liu  
China Institute of Water Resources and Hydropower Research,  
Beijing 100048, China

W. Song · H. Liu  
China Research Center on Flood & Drought Disaster Reduction of  
the Ministry of Water Resources, Beijing 100038, China

J. Jiao (✉)  
China Institute of Hydropower and Water Research,  
Beijing 100048, China  
e-mail: 68283847@qq.com

district that lack of observation data. In particular, the soil conservation service curve number (SCS-CN, 1972) model, which was developed by the United States Department of Agriculture (USDA) based on climate characteristics and hydrological runoff data from the USA, has a simple structure and fewer required parameters and is thus widely used to predict rainfall surface runoff (Li et al. 2015).

The SCS-CN model has two important parameters: (1) the initial loss rate  $\lambda$  before the appearance of surface runoff, including ground filling, intercepting, and permeation and (2) the SCS-CN, which comprehensively reflects different indicators of surface runoff capacity of different land uses and land cover combinations. Studies have shown that CN (i.e., curve number) is the most sensitive parameter in the SCS-CN model, as a 10% change in this parameter may result in a 45 to 55% error in the simulation results (Boughton 1989). Because CN is affected by many factors such as land use and management, soil characteristics, slope, and pre-existing water content, CN often varies widely between different runoff events with the same land use and land cover conditions (Nigam et al. 2017).

When the SCS-CN model manual was first published in 1972, it was divided into four types (A, B, C, and D) according to soil infiltration capacity. Moreover, CN values could be obtained from a table in the model manual, according to different land use and land cover values for each soil type. Furthermore, the antecedent moisture condition (AMC) was divided into three conditions based on the rainfall in 5 days prior to the surface runoff: “dry” (AMC I), “average” (AMC II), and “wet” (AMC III). Researchers have since carried out many studies on the effect of slope, soil characteristics, and soil water content on CN value; analyzed the influence of these factors on CN; and proposed equations to calculate CN using slope and AMC (Sharpley and Williams 1990; Huang et al. 2007; Ajmal et al. 2016; Lal et al. 2017; Choi et al. 2019). The latest version of the SCS-CN model manual indicates that these factors are uniformly attributed to preexisting conditions (NRCS 2009). However, current research has focused on the effects of surface features on CN values (Hosseini and Mahjouri 2018). The effect of rainfall processes on runoff events has also been found to be very significant. For example, runoff could be significantly different for two rainfall events with the same rainfall amount (30 mm) but different durations (1 and 24 h). Since the publication of the SCS-CN model, only one parameter

(CN) reflected rainfall characteristics, and the characteristics of the rainfall process could not be reflected by it, which may lead to simulation deviations.

In the 1990s, researchers began to simulate runoff events in China with the SCS-CN model. Importantly (Mu 1992; Wei and Xie 1992), the model's  $\lambda$  and CN values were revised and optimized to improve its simulation accuracy, and the soil characteristics of China were considered based on observed rainfall and runoff data. For instance, Fu et al. (2011) optimized the  $\lambda$  value for the Loess Plateau, Shi et al. (2009) calculated the variation range of  $\lambda$  in the Three Gorges Reservoir Region of the Yangtze River, and Chen et al. (2014) revised the  $\lambda$  value for sloped croplands with purple soil. Regarding the CN value, Luo et al. (2002) calculated this parameter for different surfaces of the Loess Plateau, Huang et al. (2006, 2007) analyzed the influence of slope and soil moisture content of different soil layer depths on the CN value, and Fu et al. (2013) assigned calculated CN values to different hydro-soil groups and land uses in Beijing. These studies mainly employed observation data to revise the key SCS-CN model parameters; however, verification and systematic improvement methods for the model are scarce due to a lack of long time series observation data.

The mountainous area of Beijing is an important source of surface drinking water in the region. Although the city government has made great progress in ecological construction and environmental protection, in some areas, soil erosion is still very prominent due to the concentration of agricultural production and infrastructure activities, especially in steep slopes (Li et al. 2013), which directly threatens the quality of surface drinking water sources such as the Miyun Reservoir (Jiao et al. 2015). Thus, accurate simulation of runoff is very important for the analysis of sediment and water-pollutant transport. In recent years, researchers have attempted to use the SCS-CN model to predict the surface runoff in this area. Fu et al. (2013) calculated the CN values of different hydro-soil groups and under surface coverage by analyzing rainfall–runoff data from 64 slope runoff areas. However, the SCS-CN model has not been optimized to calculate surface runoff in this area. Moreover, although measured rainfall–runoff data were used to decrease the variation of CN value, the SCS-CN for each runoff event ( $CN_t$ ) still varied widely (i.e., the maximum value could be more than three times higher than the minimum) even in the same community land-use management mode. These deviations were largely

attributed to the implementation of a total CN average value for all the runoff events in the simulations, instead of accounting for individual rainfall event variations. Surface runoff is not only affected by rainfall amount but also by rain intensity, rain patterns, and other factors. The mountainous area of Beijing exhibits large terrain fluctuation, as well as strong local convection and frontal activity, which are the primary drivers of rainstorms. Thus, if the influence of rainfall process on runoff is not considered, model prediction error may increase. In view of this, on the basis of taking account of the effect of rainfall process and characteristics on surface runoff, especially the variation of rainfall intensity, our study accounted for the effect of rainfall processes and characteristics on surface runoff and flow by proposing an SCS-CN calculation method for each runoff event (CN<sub>t</sub>), making the model suitable to characterize drinking water dynamics in Beijing.

**Materials and methods**

Overview of the study area

The Shixia watershed in Miyun County is located north-east of the Miyun Reservoir, approximately between and 47° 32' N–47° 38' N and 117° 01' E–117° 07' E; it has a drainage area of 33 km<sup>2</sup> and is located in the lower reaches of the Chaohe River Basin (Fig. 1a). The watershed is a shallow rocky/hilly terrain with an altitude of 160 to 353 m. The main rock and soil types in the basin are gneiss and brown soil, respectively, and the region exhibits a warm temperate monsoon climate. The average annual precipitation is 660 mm, and the rainfall from June to September accounts for approximately 75% of the annual rainfall.

Observation data and methods

To optimize and evaluate the SCS-CN model, 253 rainfall and runoff event data were measured in seven sloped runoff plots (Table 1) in the Shixia watershed. Rainfall was measured with a bucket rain gauge with a 0.1-mm resolution. The basic information and soil properties of each plot are summarized in Table 1. The seven plots were chosen because their land use and management practices have remained unchanged for at least 10 years. Among them, the land use and management mode of plots 1, 2, 3, 4, and 7 remained unchanged from 1994 to

2015, and those of plots 5 and 6 remained unchanged from 2003 to 2015. Rainfall and runoff data from 1994 to 2000 were used to improve the SCS-CN in five plots, including plots 1, 2, 3, 4, and 7. As the observation of surface runoff began in 2003, data from rainfall–runoff events from 2003 to 2005 were used to optimize the SCS-CN model in plots 5 and 6. Data from 149 rainfall–runoff events were used to optimize the SCS-CN model in total. The simulation performance of the improved model was assessed with data from 104 rainfall–runoff events for all of the plots from 2013 to 2015.

This study measured the surface soil moisture content of plots 1, 2, 3, 4, and 5 in 2015. A soil moisture conductivity sensor (HydraProbe II SDI-12, Stevens Water) was used to measure the soil moisture content at a 10- and 30-cm depth, and the average value of the two is the moisture content of the soil surface at 30 cm (volume ratio, dimensionless). The measurements were taken at 30-min intervals. Therefore, the moisture content in the top 30 cm of soil was obtained 30 min before the rainfall ( $\theta_0$ ), during the rainfall, and 30 min after the rainfall ( $\theta_t$ ). Moreover, the maximum moisture content during the rainfall ( $\theta_{max}$ ) was identified.

Optimized SCS-CN method

Overview

The SCS-CN method (US Department of Agriculture 1972) is based on the principle of water balance (Eq. 1) and two basic assumptions. The first assumption is that the ratio of direct runoff to maximum potential runoff is equal to the ratio of infiltration to potential maximum hold (Eq. 2); the second assumption is that the initial loss is proportional to the potential maximum hold (Eq. 3):

$$P = I_a + F + Q \tag{1}$$

$$Q/(P-I_a) = F/S \tag{2}$$

$$I_a = \lambda \cdot S \tag{3}$$

In the equations above,  $P$  represents rainfall (mm),  $I_a$  is the initial loss (mm),  $F$  is the observed holding amount (mm),  $Q$  is the surface runoff (mm),  $S$  is the potential water storage capacity (mm), and  $\lambda$  is the

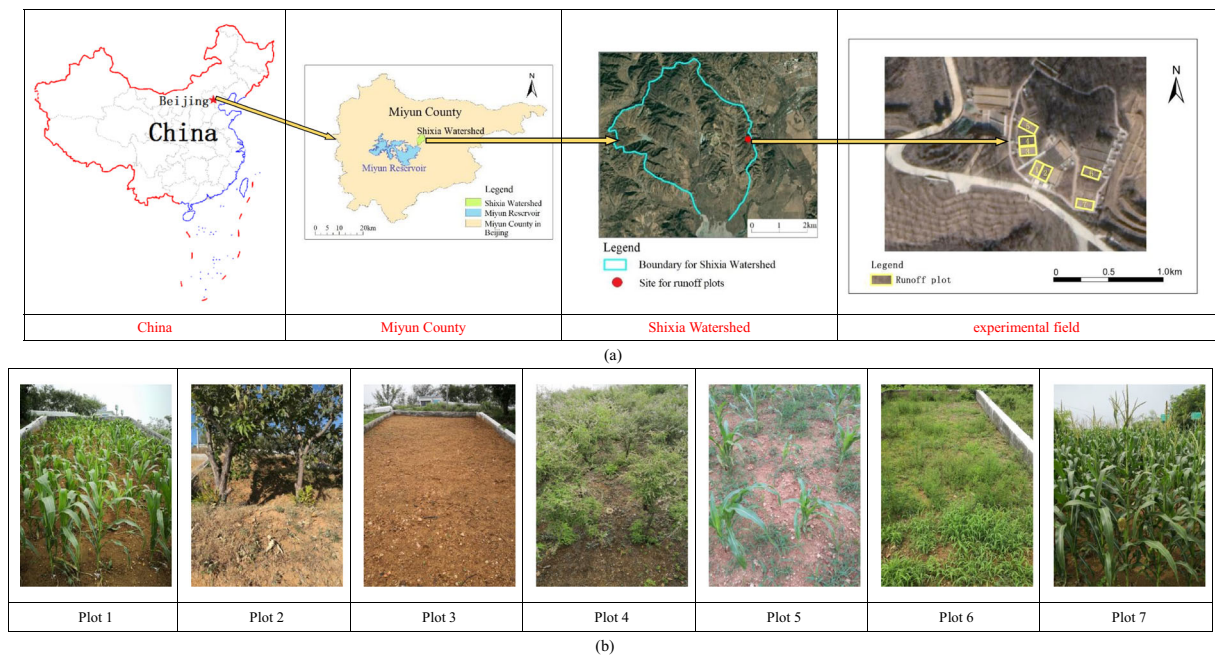


**Fig. 1** Location of the experimental field and distribution of the plots (a) and photographs for the plots (b)

initial loss rate. Equations (1) to (3) can then be combined with  $Q$  to obtain Eq. (4):

$$Q = \frac{(P - \lambda S)^2}{P + (1 - \lambda)S}, \quad (P > \lambda S)$$

$$Q = 0, \quad (P \leq \lambda S)$$
(4)

For practicality,  $S$  can be calculated using CN as follows:

$$S = 25400 / CN - 254, \quad 0 < CN \leq 100$$
(5)

Using observation data, the values of  $P$  and  $Q$  can be obtained with Eq. (6), which is inversely deduced from Eqs. (4) and (5). The CN value is then determined with Eq. (7):

$$S = \frac{2\lambda P + (1 - \lambda)Q - \sqrt{4QP\lambda^2 + (1 - \lambda)^2 Q^2 + 4\lambda(1 - \lambda)QP}}{2\lambda^2}$$
(6)

$$CN = 25400 / (254 + S)$$
(7)

The CN value is first determined according to hydrological soil groups; the SCS manual is then used to obtain the  $CN_2$  values under different land-use conditions. According to cumulative precipitation over 5 days prior to the surface runoff, the AMC is sub-classified

(Table 2) into AMC I, AMC II, AMC III to describe dry, average, and wet conditions, respectively.  $CN_1$  and  $CN_3$  can be calculated based on the equations provided by  $CN_2$  using the SCS manual. The US Soil Conservation Service divides soil into four major types (A, B, C, and D), according to soil infiltration capacity in the decreasing order (USDA 1972). The main hydrologic soil group in the mountainous area of Beijing is class B, and the soil AMC in the region is mostly dry. In order to make the results more practical, the runoff curve value under AMC I (i.e.,  $CN_1$ ) was adopted as the runoff prediction parameter in our study.

#### SCS-CN calculation method for each runoff event ( $CN_t$ )

During the rainfall process, the concentration of rainfall events over time has an important impact on the surface runoff and soil erosion process (Wischmeier and Smith 1978; Wilken et al. 2018; Wu et al. 2018). Thus, our study sought to use the ratio of the maximum rainfall for a certain duration ( $X_{min}$ ) to the total rainfall amount for the event ( $P_X/P$ ) to reflect the rainfall intensity over time, where  $X$  is the duration (min) corresponding to the maximum rainfall, and  $X = 5, 10, 15, 20, 30, 40, 50,$  and  $60$  min. Based on previous research findings (Shi et al. 2009; Fu et al. 2011; Xiao et al. 2011; Lal et al. 2017), the  $\lambda$  parameter in the SCS-CN model developed

**Table 1** Features for plots in Shixia watershed

Plot label	Slope (°)	Slope length (m)	Slope width (m)	Land use	Land management	Runoff event frequency	pH value	Mechanical composition (%)				0.002–0.02 mm < 0.002 mm
								0.25–2 mm	0.05–0.25 mm	0.02–0.05 mm	0.002–0.02 mm	
1	16.8	10	5	Cultivated land	Corn	53	6.05	51.21	28.91	4	8	7.88
2	16.8	10	5	Arboreal land	Chestnut tree	29	6.48	59.90	22.22	6	6	5.88
3	14.6	10	5	Bare land	Vegetation cover <5%	51	6.61	54.27	25.85	4	8	7.88
4	14.6	10	5	Shrub land	Vegetation cover 45–60%	25	6.12	61.16	20.96	6	6	5.88
5	11.6	10	5	Cultivated land	Corn	31	6.32	48.95	30.72	7	5	8.33
6	19.0	10	5	Grass	Vegetation cover 30%	21	6.59	64.21	19.91	6	2	7.88
7	3.8	10	5	Cultivated land	Slow slope planting Corn	43	6.10	30.23	43.89	8	8	9.88

**Table 2** Classification of antecedent soil moisture condition (AMC)

AMC	Cumulative precipitation over 5 days (mm)	
	Dormant season	Growing season
I	<12.7	<35.6
II	12.7–27.9	35.6–53.3
III	>27.9	>53.3

herein was assigned a value range from 0 to 0.30 at 0.01 intervals. When combined with the observed rainfall and runoff data from runoff events, a SCS-CN can be calculated for each runoff event (CN<sub>t</sub>) and for each plot with Eqs. (6) and (7), with CN<sub>1</sub> being the average value of the curve number for each runoff event. Afterward, the functional relationship between the ratio of CN<sub>t</sub> to CN<sub>1</sub> (CN<sub>t</sub>/CN<sub>1</sub>) and P<sub>X</sub>/P for rainfall events was analyzed with Eq. (8). Then, the method to calculate CN<sub>t</sub> with the rainfall intensity degree over time was applied to the improved SCS-CN model:

$$(CN_t/CN_1) = f(P_X/P) \tag{8}$$

In the equation, P<sub>X</sub> and P are the maximum rainfall (X<sub>min</sub>) and the total rainfall amount (in mm) during the rainfall, respectively.

*Determination of initial loss ratio and assessment of the simulation performance of the optimized model*

The simulation performance of the model was compared at different λ and X values, after which optimal λ and X values were selected. The Nash model efficiency coefficient E<sub>f</sub> (Nash and Sutcliffe 1970), correlation coefficient (r), and mean relative error (MRE) were used to compare the predicted and observed runoff depth and to test the simulation performance of the optimized model. These values were calculated as follows:

$$E_f = 1 - \frac{\sum_{i=1}^n (Q_{ob} - Q_{cal})^2}{\sum_{i=1}^n (Q_{ob} - Q_{oba})^2} \tag{9}$$

$$MRE = \frac{\sum_{i=1}^n (Q_{cal} - Q_{ob})}{\sum_{i=1}^n Q_{ob}} \tag{10}$$

where Q<sub>ob</sub> is the observed runoff depth (mm), Q<sub>cal</sub> is the predicted runoff depth (mm), Q<sub>oba</sub> is the average of



all observed runoff depths (mm), and  $n$  is the number of total runoff events.

## Results

### Calculated $CN_t$ values and their variations

Figure 2 illustrates the ratio of the maximum and minimum  $CN_t$  values and its variation coefficient (Cv) under different  $\lambda$  values for each runoff plot. It can be observed that even in the plots where land use and management methods remain unchanged throughout the year, the range between  $CN_t$  values from different runoff events is still very significant. Although the maximum to minimum  $CN_t$  value ratio and Cv gradually decreased as  $\lambda$  increased, even when the value of  $\lambda$  is 0.3 (i.e., the maximum assigned  $\lambda$  value in this study), the maximum to minimum  $CN_t$  value ratio for arboreal land (Plot 2), shrubland (Plot 4), and low-slope farmland (Plot 7) was still  $>2.0$ , while the ratio for other land uses was  $>1.5$ . Moreover, when  $\lambda \leq 0.05$ , the ratio for arboreal land, shrubland, and low-slope farmland was  $>4.5$ , and that of other plots was  $>2.5$  (Fig. 2a). Cv value changes followed a similar trend to those observed for the maximum to minimum  $CN_t$  value ratio (Fig. 2b). The variation between  $CN_t$  values for different runoff events was more significant in plots with high vegetation coverage. Studies have shown that a 10% change in CN value may result in a 45% to 55% error in the calculation results (Boughton 1989). Here, substantial simulation errors were observed if the various SCS-CN values for different

rainfall and runoff events were not taken into account (i.e., if only a global average was used) when simulating runoff in the mountainous area of Beijing.

### Influence of rainfall characteristics on $CN_t$

According to the observed rainfall–runoff data, there is a significant positive correlation between  $CN_t/CN_1$  and  $P_X/P$  that is significant at the 0.01 level (Table 3). When  $X = 20$  min, the correlation coefficient  $r$  was the highest, and  $r$  varied between 0.636 and 0.686 at different  $\lambda$  values, with an average of 0.679. When  $X = 15$  min and  $X = 30$  min,  $r$  varied narrowly between 0.621 and 0.677 at different  $\lambda$  values, with an average of 0.668. When  $X = 10$  min and  $X = 40$  min,  $r$  varied between 0.611 and 0.658 under at  $\lambda$  values, with an average of 0.651. When  $X = 50$  min and  $X = 60$  min,  $r$  varied between 0.585 and 0.634 at different  $\lambda$  values, with an average of 0.627. When  $X = 5$ , the correlation coefficient was lowest, and  $r$  varied from 0.549 to 0.611 at different  $\lambda$  values, with an average of 0.602. The  $X$  value changes between 5 and 60 had no significant effect on the correlation between  $CN_t/CN_1$  and  $P_X/P$  (Table 3). Moreover,  $CN_1$  remained unchanged in surfaces with the same land use and management mode, and  $CN_t$  increased accordingly with  $P_X/P$ , indicating that the rainfall concentration degree over time has a significant impact on  $CN_t$ .

Based on the aforementioned analysis, our study proposes an equation to calculate  $CN_t$ , whereby  $P_X/P$  is the independent variable. However,  $CN_t$  may be more than 100 if  $P_X/P > 95\%$ , for the linear equation;

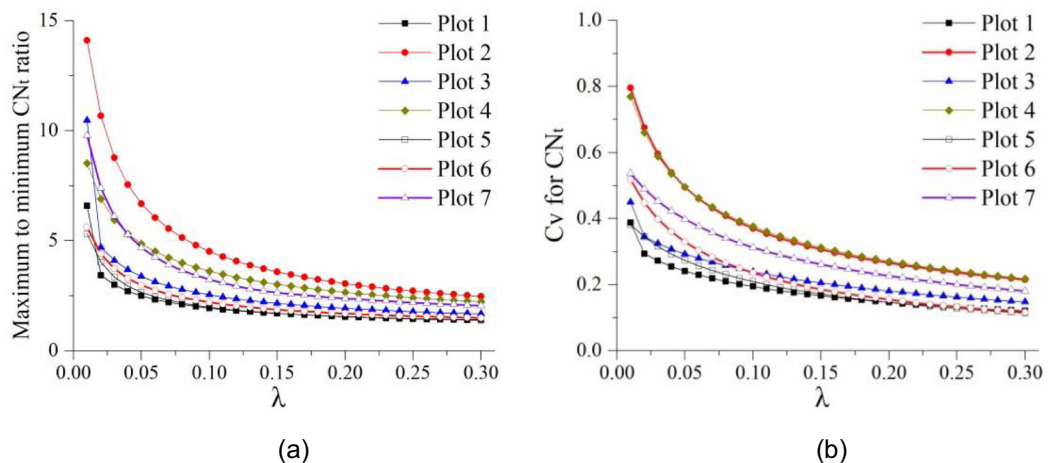


**Fig. 2** Maximum to minimum  $CN_t$  value ratio for each plot (a) and its variation coefficient (b)

therefore, a power function equation was adopted to calculate  $CN_t$  (Eq. 11):

$$CN_t = CN_1 \cdot a \cdot (P_x/P)^b, CN_t \leq 100 \quad (11)$$

Optimized SCS-CN model simulation performance

In this study, the runoff depth predicted by the improved SCS-CN model was compared with the observed runoff volume under different  $\lambda$  and  $X$  values. The efficiency

factor of the improved model ( $E_f$ ) decreased as  $\lambda$  increased (Fig. 3a), and the best simulation performance was achieved when  $\lambda$  equaled 0.01 or 0.02, at a fixed  $X$  value. In terms of maximum rainfall periods, when  $\lambda \geq 0.10$ ,  $E_f$  was the lowest when  $X=60$  min or 50 min, followed by  $E_f$  when  $X=40$  min.  $E_f$  then increased significantly when  $X \leq 30$ , and differences between  $X$  values had little effect on  $E_f$  in this range. Moreover,  $E_f$  was highest when  $\lambda < 0.10$  and  $X=5$  min. The correlation coefficient ( $r$ ) trend between observed and predicted values was similar to the  $E_f$  trend (figure not shown),

**Table 3** Correlation coefficient ( $r$ ) between  $CN_t/CN_1$  and  $P_x/P$

$\lambda$	Xmin for $P_x/P$							
	5	10	15	20	30	40	50	60
0.01	0.549	0.618	0.625	0.636	0.621	0.611	0.589	0.585
0.02	0.565	0.631	0.639	0.651	0.638	0.626	0.603	0.600
0.03	0.576	0.641	0.650	0.663	0.650	0.636	0.614	0.611
0.04	0.584	0.648	0.656	0.670	0.657	0.643	0.620	0.618
0.05	0.590	0.649	0.660	0.674	0.662	0.646	0.623	0.621
0.06	0.594	0.652	0.664	0.677	0.666	0.649	0.626	0.625
0.07	0.598	0.654	0.666	0.680	0.669	0.651	0.628	0.627
0.08	0.601	0.656	0.668	0.682	0.671	0.653	0.630	0.629
0.09	0.603	0.657	0.670	0.683	0.673	0.655	0.631	0.631
0.10	0.605	0.658	0.671	0.685	0.675	0.655	0.632	0.632
0.11	0.606	0.658	0.671	0.685	0.676	0.656	0.632	0.633
0.12	0.608	0.658	0.672	0.686	0.676	0.656	0.633	0.633
0.13	0.609	0.658	0.672	0.686	0.677	0.657	0.633	0.634
0.14	0.609	0.658	0.672	0.686	0.677	0.657	0.633	0.634
0.15	0.610	0.658	0.672	0.686	0.677	0.657	0.633	0.634
0.16	0.610	0.658	0.672	0.686	0.677	0.656	0.633	0.634
0.17	0.611	0.658	0.672	0.686	0.677	0.656	0.632	0.634
0.18	0.611	0.657	0.671	0.685	0.677	0.656	0.632	0.634
0.19	0.611	0.657	0.671	0.685	0.677	0.655	0.632	0.633
0.20	0.611	0.656	0.671	0.685	0.677	0.655	0.631	0.633
0.21	0.611	0.656	0.670	0.684	0.676	0.654	0.631	0.633
0.22	0.611	0.655	0.670	0.684	0.676	0.654	0.630	0.632
0.23	0.611	0.655	0.669	0.683	0.676	0.653	0.630	0.632
0.24	0.611	0.654	0.668	0.682	0.675	0.653	0.629	0.631
0.25	0.610	0.653	0.668	0.682	0.675	0.652	0.629	0.631
0.26	0.610	0.653	0.667	0.681	0.674	0.652	0.628	0.630
0.27	0.610	0.652	0.667	0.681	0.674	0.651	0.627	0.630
0.28	0.610	0.651	0.666	0.680	0.673	0.650	0.627	0.629
0.29	0.609	0.651	0.665	0.679	0.673	0.650	0.626	0.629
0.30	0.609	0.650	0.665	0.679	0.672	0.649	0.626	0.628

Positive correlations are all significant at the 0.01 level

and MRE increased accordingly with  $\lambda$  increases in the improved SCS-CN model (Fig. 3b); MRE only varied between  $-10$  and  $10\%$  when  $\lambda \leq 0.05$ .

For plots 1, 2, 5, and 7,  $E_f$  and  $r$  reached maximum values (i.e., optimal simulation results) when  $\lambda = 0.01$  and  $X = 5$  min (Table 4). The total number of the runoff events for the four plots accounted for 64.4% of all runoff events and 68.9% of the total runoff amount. The runoff simulation performance for plots 3 and 6 was optimal when  $\lambda = 0.01$  and  $X = 10$  min, and runoff simulation for plot 4 was optimal when  $\lambda = 0.03$  and  $X = 20$  min.

For practicality, constant values were assigned to  $\lambda$  and  $X$  in the improved SCS-CN model. Overall, the improved model simulation performance was ideal when  $\lambda$  was equal to 0.01 and 0.02. When  $\lambda = 0.01$  and  $X = 5$  min,  $E_f$  and  $r$  reached the maximum values of 0.791 and 0.895, respectively. At this point, the MRE was only  $-5.09\%$ . Therefore,  $\lambda$  was assigned the value of 0.01 in the improved model to maximize  $E_f$ , and  $P_5/P$  was selected as the variable to describe the degree of rainfall concentration over time. Furthermore, the optimal  $\lambda$  and  $X$  values were not significantly different from those of each plot (Table 4), and the unified value of  $E_f$  was found to be only 0.02 less than that of each cell. Values of  $CN_1$ ,  $a$ , and  $b$  for each runoff plot are summarized in Table 5.

The SCS manual suggests using a  $\lambda$  value of 0.20 when applying the CSC-CN model, because this value results in a more uniformly distributed rainfall simulation throughout the year (Wilson et al. 2017), accounting for approximately 70% of rainfall infiltration into the soil. However, regions with monsoon climate exhibit abrupt seasonal rainfall changes, with heavy rain events, and significantly lower soil infiltration.

Therefore,  $\lambda$  was assigned a value of no more than 0.05 in our study (Ajmal et al. 2016).

In this study, the observed runoff was compared with the runoff predicted by the model prior to optimization (Fig. 4). A significant difference in simulation accuracy was observed between the optimized and non-optimized models. Particularly, the maximum  $E_f$  value was only 0.05 in the non-optimized model, and  $E_f$  was less than 0 when  $\lambda$  was 0.02;  $r$  was also significantly reduced. Figure 4 illustrates the comparison between the predicted and observed values of the optimized (Fig. 4a) and non-optimized (Fig. 4b) models when  $\lambda = 0.01$ . Overall, the values predicted by the non-optimized model notably deviate from the 1:1 line indicated in red in Fig. 4. This illustrates that significant prediction errors occur when the influence of rainfall characteristics and intensity are not considered in the study region.

Effect of different factors on the simulation performance of the optimized CSC-CN model

#### Antecedent soil moisture conditions

This study analyzed the simulation performance of the improved CSC-CN model for runoff events at different soil AMCs. AMC I, AMC II, and AMC III conditions during 2013–2015 were observed in 66%, 28%, and 6% of all runoff events, respectively. Notably, AMC I accounted for most of the soil moisture conditions in the studied period, and high-slope yield flow during AMC I conditions was mainly attributed to over-seepage; rainfall intensity is also an important factor mediating runoff volume. The optimized model accounted for the effect of maximum rain intensity periods on runoff generation but did not directly use

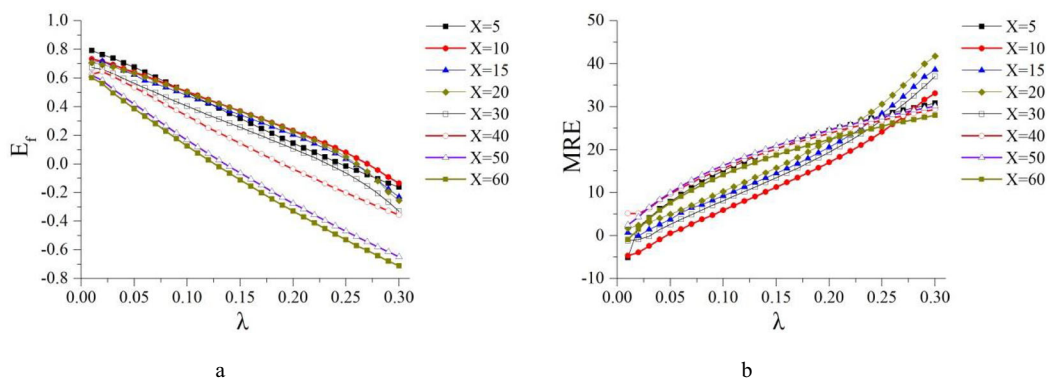


**Fig. 3**  $E_f$  (a) and mean relative error (MRE) (b) for the improved SCS-CN model



**Table 4** Optimal simulation performance of the optimized SCS-CN model for each plot

Plot label	Land use	Annual flow times from 2013 to 2015	Land use	Value for parameters				Simulation results			
				$\lambda$ Initial abstraction ratio	X Maximum period	CN <sub>i</sub> Average curve number	a for Eq. 11	b for Eq. 11	$E_f$	r	MRE (%)
1	Cultivated land	23	Steep-slope corn	0.01	5	60.15	1.861	0.304	0.886	0.944**	-6.04
2	Arboreal land	5	Chestnut trees	0.01	5	32.41	2.047	0.430	-7.56	0.743	67.21
3	Bare land	21	Vegetation cover <5%	0.01	10	54.33	1.875	0.468	0.890	0.945**	-0.01
4	Shrub land	7	Vegetation cover 45–60%	0.03	20	27.15	1.570	0.423	-2.39	0.770*	-55.31
5	Cultivated land	21	Steep-slope corn	0.01	5	52.53	2.834	0.527	0.776	0.913**	3.62
6	Grassland	9	Vegetation cover 30%	0.01	10	46.31	1.813	0.458	0.603	0.852**	15.26
7	Cultivated land	18	Low-slope corn	0.01	5	50.56	2.769	0.561	0.727	0.891**	-19.21
Total				-	-	-	-	-	0.811	0.905**	-3.07

\*, \*\* indicate significant at the 0.01 and 0.05 level, respectively

the rainfall intensity as a model variable. Thus, the accuracy of the runoff simulation under AMC I conditions decreased ( $E_f = 0.649$ ;  $r = 0.817$ ; MRE = 9.12%; Fig. 5a). However, the improved model has relatively high accuracy for runoff simulation under AMC II and III conditions ( $E_f = 0.883$ ;  $r = 0.942$ ; MRE = 5.6%). Under these conditions, the soil moisture content was relatively higher. Soil moisture content during runoff is more likely to approach or reach field water capacity, and both over-infiltration runoff and stored-full runoff may occur. Moreover, rainfall has a more significant impact on runoff amount when the soil moisture content is low.

*Land use*

This study also analyzed the accuracy of the optimized model to simulate runoff events when accounting for different land use types (Fig. 5b); the selected parameters are summarized in Table 5. The simulation results of this model were satisfactory ( $E_f = 0.831$ ;  $r = 0.922$ ; MRE = 13.67%) for bare land (plot 3) and cultivated land plots (plots 1, 5, and 7;  $E_f = 0.828$ ;  $r = 0.916$ ; MRE = 6.50%). Rills are easily created on exposed surfaces during rainfall events and become narrow ditches or grooves with repeated rainfall. However, corn cultivation management practices such as weed control result in large bare areas, which accelerates rill erosion. Moreover, increases in slope bare surface result in reduced brown soil, and increases in the number, length, and width of fine grooves facilitate the formation of a more stable convection path.

The simulation accuracy of the optimized model was lower for grassland runoff ( $E_f = 0.439$ ;  $r = 0.808$ ; MRE = 19.31%). Even during the rainy season, the vegetation cover of grasslands varies greatly. At the beginning of the rainy season, weeds begin to grow. At this time, the ground vegetation coverage is only approximately 5% and reaches its highest values (40–50%) in mid- to late-August. The optimized model did not illustrate the effect of vegetation cover on CN<sub>i</sub> over short time periods, thus reducing its simulation accuracy.

The production of grass surface crust also has an impact on the runoff process. If  $P_{10}/P$  is used as a variable to simulate runoff depth and  $\lambda$  is still equal to 0.01, the predicted values exhibit an  $E_f$ ,  $r$ , and MRE of 0.603, 0.852, and 15.26%, respectively (Table 4), and the simulation performance is significantly improved. The splashing effect of raindrops requires some time to

**Table 5** Parameters for the optimized SCS-CN model

Plot label	Land use	Land use	Parameter values			
			$\lambda$ Initial abstraction ratio	$CN_1$ Average curve number	$a$ $a$ for Eq. 11	$b$ $b$ for Eq. 11
1	Cultivated land	Steep-slope corn	0.01	60.15	1.861	0.304
2	Arboreal land	Chestnut trees	0.01	32.41	2.047	0.430
3	Bare land	Vegetation cover <5%	0.01	54.33	2.007	0.398
4	Shrub land	Vegetation cover 45–60%	0.01	27.15	2.206	0.446
5	Cultivated land	Steep-slope corn	0.01	52.53	2.834	0.527
6	Grassland	Vegetation cover 30%	0.01	46.31	2.164	0.416
7	Cultivated land	Low-slope corn	0.01	50.56	2.769	0.561

erode the decomposing crust; therefore, assuming slightly longer periods of maximum rainfall could allow for more effective monitoring of the effect of rainfall on surface flow production.

The optimized model is not ideal for the simulation of flow production on arboreal land. From 2013 to 2015, arboreal (plot 2) and shrub lands (plot 4) produced runoff on 12 occasions, and the  $E_f$  predicted by the model was only  $-3.03$ . Thus, these plots only accounted for 11.5% of all yield events. Moreover, the averaged runoff depth was only 3.68 mm, which is 47.0% of the average value of other plots. Therefore, the simulation error of arboreal and shrub land plots had no significant influence on the overall simulation performance of all runoff events. It should be noted that this study used rainfall–runoff data from 1994 to 2000 to

optimize the model and assessed its simulation performance with rainfall–runoff data from 2013 to 2015; however, the runoff coefficients in these two periods are significantly different. Plot 2 decreased from 0.057 in 1994–2000 to 0.032 in 2013–2015, and plot 5 increased from 0.058 to 0.140 in the same periods. The growth and development of plant roots and the formation and decomposition of the litter layer contribute to the gradual improvement of soil physical and chemical properties. Furthermore, the content of organic matter and humus, as well as root activity, can increase soil porosity and improve permeability. Additionally, the interannual variation of plant canopy characteristics is also an important factor affecting surface runoff changes (i.e., less vegetation cover leads to more surface runoff). The runoff mechanisms in arboreal land are relatively

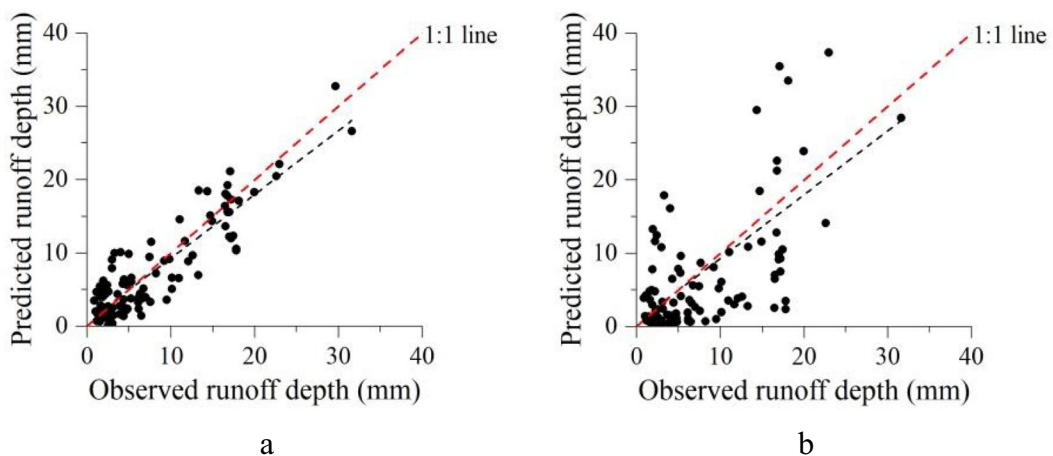


**Fig. 4** Comparison between observed runoff and predicted runoff simulated by the optimized and non-optimized SCS-CN models. **a** Optimized SCS-CN model. **b** Non-optimized SCS-CN model. Note: The dotted line in the figure represents the data point linear trend

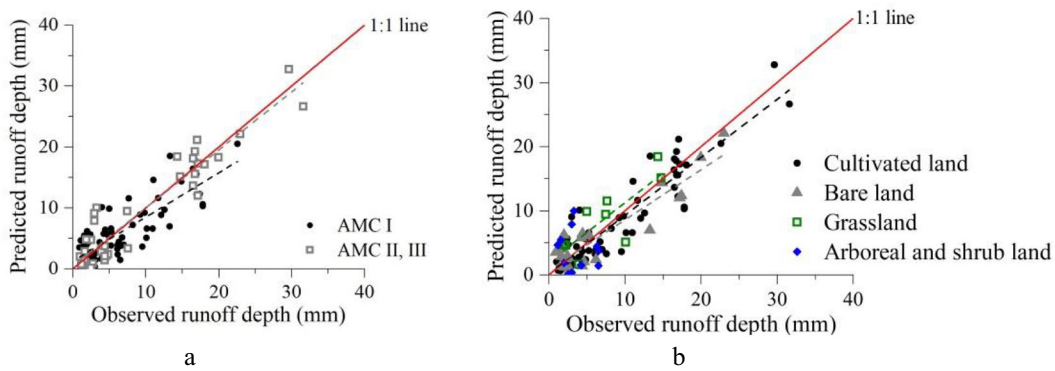


**Fig. 5** Comparison between observed and predicted runoff calculated by with the optimized SCS-CN model under different AMCs and land use scenarios. **a** Different AMC. **b** Different land use. Note: The dotted line in the figure represents the data point linear trend

complex, as over-infiltration and over-holding may occur under specific rainfall conditions. Therefore, the model parameter optimization method described herein should be developed further to allow for an in-depth analysis of the mechanisms of runoff and yield.

**Discussion**

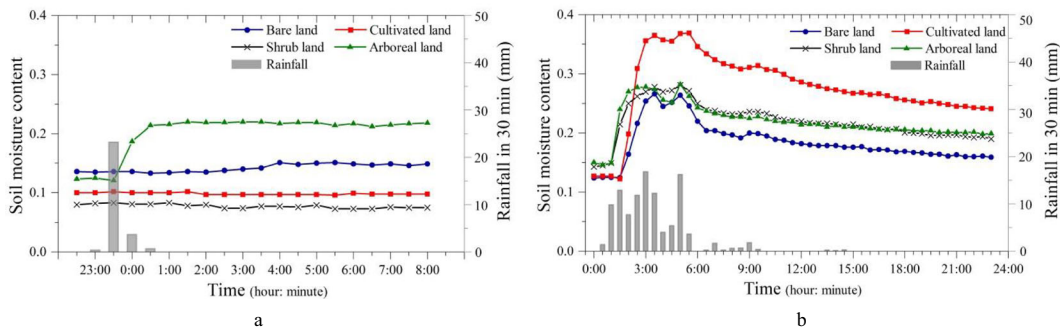
Effect of soil moisture content on  $CN_t$

Table 6 summarizes the moisture content variation range in the soil surface layer (i.e., 30 cm depth) during runoff events with different rainfall duration. Overall, with increased rainfall duration, the ratio of  $\theta_{max}$  to  $\theta_0$  ( $\theta_{max}/\theta_0$ ) gradually increased as well. For runoff production events that lasted less than 4 h, the soil moisture content during rainfall increased by only 29% at the highest level and by 8% on average. The surface flow

production caused by short-term rainfall was notably in the form of over-permeability; in other words, surface flow production occurred when the runoff generation rate was greater than the infiltration rate. For example, during the rainfall of August 28, 2015 (Fig. 6a), the total rainfall amount was 27.8 mm, the rainfall duration was 1.63 h, and the maximum 5- and 30-min rainfall intensity was 136.8 and 51.2 mm/h, respectively. During this rainfall event, only the soil surface moisture content of forest trees increased significantly, and there was no significant increase in soil surface moisture content in plots with other land uses. The runoff coefficient of arboreal land was only 7.1%, while the runoff coefficient of other land uses varied between 23.4 and 64.0%, with an average of 48.6%, indicating that surface runoff could occur even if the soil surface moisture content did not reach saturation. When rainfall lasted more than 4 h, the soil moisture content increased significantly, with an average of 49% and a maximum of 210% compared

**Table 6** Soil surface moisture content in runoff events with different rainfall durations and simulation performance of the optimized SCS-CN model

Rainfall duration (h)	Number of runoffs	Average runoff coefficient	Ranges of moisture content in the soil surface layer				Simulation effect of improved runoff curve number model		
			$\theta_0$	$\theta_{max}$	$\theta_t$	$\theta_{max}/\theta_0$	$E_f$	$r$	MRE (%)
<2	25	0.355	0.057–0.106	0.059–0.110	0.052–0.110	1.00–1.09	0.532	0.890	–35.70
$2 \leq t < 4$	25	0.249	0.107–0.182	0.121–0.195	0.122–0.190	1.01–1.29	0.780	0.885	1.32
$4 \leq t < 6$	22	0.228	0.087–0.117	0.088–0.176	0.079–0.170	1.01–1.56	0.894	0.952	–9.70
$\geq 6$	32	0.152	0.048–0.172	0.059–0.369	0.049–0.267	1.02–3.10	0.811	0.928	13.60



**Fig. 6** Changes in surface soil moisture content in typical rainfall-runoff events. **a** August 28, 2015. **b** July 19, 2015

with the soil moisture before the rainfall. The occurrence of full flow production and stored-full runoff is also significantly increased in runoff events caused by long periods of rainfall. In contrast, during the rainfall of July 19, 2015 (Fig. 6b), the total rainfall amount was 108.2 mm, the rainfall duration was 14.48 h, and the maximum 5- and 30-min rainfall intensity was 93.6 and 42.0 mm/h, respectively. During the rainfall event, the surface soil moisture content of each plot increased rapidly after the accumulated rainfall exceeded 20 mm and gradually decreased after the rainfall intensity was lower than 5 mm/h. This significant increase in soil moisture supply and infiltration resulted in a decrease in the runoff coefficient, and the runoff coefficient of different land-use modes shifted to 2.9–26.5%, with an average of only 16.3%, which was significantly lower than the runoff events on August 28th.

The effect of soil surface moisture content on  $CN_t$  before, during, and after rainfall was also analyzed. There was no significant correlation between  $\theta_0$  and  $CN_t/CN_1$  (Fig. 7a). Moreover,  $\theta_{max}$  and  $CN_t/CN_1$  exhibited a significant decrease in power function (Eq. 12);  $\theta_t$  and  $(CN_t/CN_1)$  also exhibited a significant decrease in

power function (Eq. 13). The ratio between  $\theta_{max}$  and  $\theta_0$  ( $\theta_{max}/\theta_0$ ) and  $CN_t/CN_1$  presented a more significant power function decline relationship (Fig. 7b; Eq. 14):

$$(CN_t/CN_1) = 0.539\theta_{max}^{-0.372}, r^2 = 0.333, p < 0.005 \quad (12)$$

$$(CN_t/CN_1) = 0.530\theta_t^{-0.369}, r^2 = 0.270, p < 0.005 \quad (13)$$

$$(CN_t/CN_1) = 1.352 (\theta_{max}/\theta_0)^{-0.705}, r^2 = 0.491, p < 0.001 \quad (14)$$

The parameters of Eq. (12) and power function (13) are very similar, indicating that both the soil surface moisture content during and after rainfall events can reflect the effect of rainfall on surface soil moisture recharge, which has a significant impact on the surface runoff volume. Under constant rainfall conditions, increased soil water replenishment through rainfall results in less surface runoff, which is manifested as a decrease in  $CN_t$ .

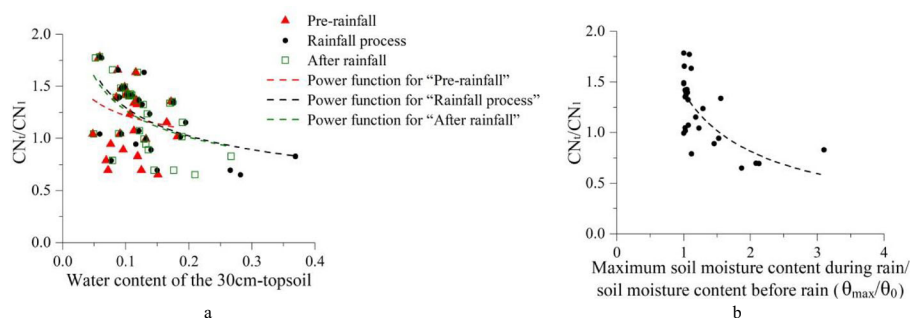


**Fig. 7** Effects of soil surface moisture content on  $CN_t/CN_1$ . **a** Relationship between water content in the first 30 cm of topsoil and  $CN_t/CN_1$ . **b** Relationship between changes in soil moisture content before and during rainfall and  $CN_t/CN_1$

CN<sub>t</sub> difference at different slopes

The equations to calculate CN in steep slopes proposed by Sharpley and Williams (1990) and Huang et al. (2006) were used as a reference to analyze plot 7 (CN = 6.6%), which had a nearly 5% slope. The annual average runoff curves for steep slope arable land areas represented by plots 1 and 5 (i.e., CN<sub>1(1)</sub> and CN<sub>1(5)</sub>) were also calculated. As illustrated in Fig. 8, the CN<sub>1(5)</sub> calculated by Sharpley and Williams equations was closer to the measured value, but the calculated CN<sub>1(1)</sub> was significantly lower than the measured value. This disagreement could be due to the fact that the equation is derived from the natural geographical conditions of the USA and thus may not be suitable to accurately describe the mountainous region of Beijing. On the other hand, the CN<sub>1(1)</sub> and CN<sub>1(5)</sub> calculated by the equations proposed by Huang et al. were significantly higher than the measured values. Studies have shown that surface runoff increases with increased slope when other conditions are kept constant (Deshmukh et al. 2013; Lal et al. 2019); however, the equations proposed by Huang et al. do not account for possible differences in the physical properties of surface soil. The soil erosion of steep-sloped arable land was found to be severe, and the average annual soil erosion for plots 1 and 5 was 7.01- and 6.20-fold higher than that of plot 7, resulting in soil particle coarsening. Furthermore, the proportion of soil particles (0.25-2 mm) in plot 1 was 20.98% higher than that of plot 7, with large amounts of gravel appearing on the surface. Soil coarseness can increase the gap between particles and surface infiltration while accordingly decreasing surface runoff. In this study, the measured

value of CN<sub>1</sub> was found to be significantly lower than the model calculation value.

It should be noted that although there are significant differences in cultivated land CN<sub>1</sub> at different slopes, there is a significant linear association between the CN<sub>t</sub> values for plots 1, 5, and 7. Therefore, the CN<sub>t(7)</sub> value of plot 7 was assigned as an independent variable, and CN<sub>t(1)</sub> and CN<sub>t(5)</sub> for plots 1 and 5 were assigned as dependent variables to fit a linear equation (Fig. 9).

Between 1994 and 2000, the relationship was:

$$CN_{t(1)} = 0.629CN_{t(7)} + 26.29, r^2 = 0.471, p < 0.001 \tag{15}$$

Moreover, the relationships between 2013 and 2015 were:

$$CN_{t(1)} = 0.648CN_{t(7)} + 30.29, r^2 = 0.703, p < 0.001 \tag{16}$$

$$CN_{t(5)} = 0.891CN_{t(7)} + 11.26, r^2 = 0.868, p < 0.001 \tag{17}$$

As observed above, there was a significant correlation between CN<sub>t</sub> in farmlands with different slopes, and with increased cultivated land planting time, the relationship between the two became more significant. Compared with Eq. (15), *r*<sup>2</sup> increased significantly in Eq. (16), which demonstrates that the similarity between the runoff processes increased after rill and inter-rill erosion in steep-sloped farmlands, as described above.

**Fig. 8** Comparison between the measured and calculated CN<sub>1</sub> values for steep-sloped farmlands

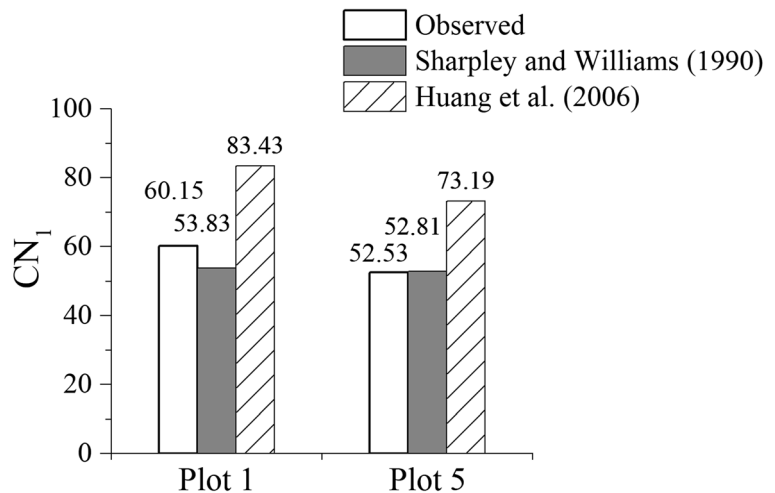
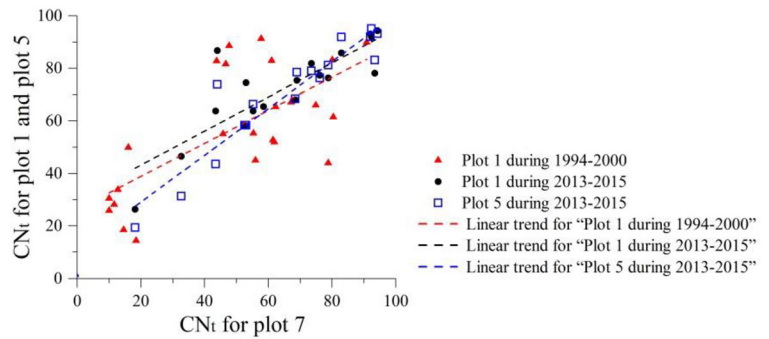




**Fig. 9** Relationship between  $CN_t$  for croplands of different slopes



In the future, the influence of slope change on  $CN_t$  in the study region should be clarified to provide a basis for  $CN_t$  calculation in steep-sloped areas.

Effect of rainfall duration on the simulation performance of the optimized SCS-CN model

According to the measured rainfall–runoff data, there is a significant power function decreasing relationship between  $CN_t/CN_1$  and rainfall duration ( $t$ ; Fig. 10). When  $\lambda = 0.01$ , the relationship is:

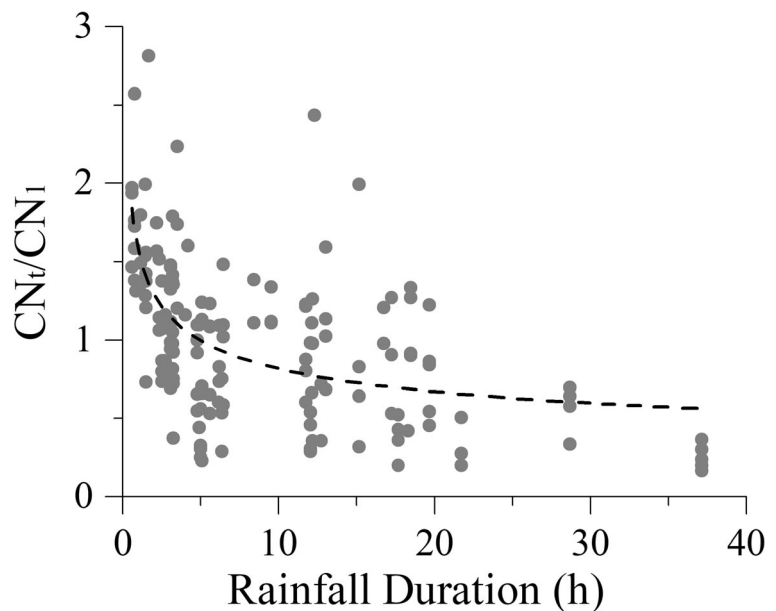
$$CN_t/CN_1 = 1.539t^{-0.332}, r^2 = 0.324, p < 0.001 \quad (18)$$

However, the determination coefficient of the function equation between them was significantly lower than

the fitting effect between  $CN_t/CN_1$  and  $P_x/P$  and was thus not used as a variable in the improved runoff curve number equation. However,  $t$  may represent the characteristics of different types of rainfall, as discussed below.

The types of rainfall that cause surface runoff in the mountainous regions of Beijing can be divided into three categories: short duration and high-intensity rainstorms caused by local strong convection conditions, from frontal rainfalls and local thunderstorms of medium duration, medium-intensity rainstorms, and long duration and low-intensity rainstorm caused by frontal rainfalls. For runoff events lasting  $t \geq 2$  h, the simulation performance of the optimized SCS-CN model was significantly improved (Table 6). The runoff coefficient of runoff production events lasting  $t < 2$  h was significantly higher (Table 6), indicating that the proportion of initial

**Fig. 10** Relationship between ( $CN_t/CN_1$ ) and rainfall duration



rainfall loss was relatively low. The  $\lambda$  value for the optimized model was constant, which was likely to have a substantial effect on the prediction of said initial rainfall loss, resulting in a low predicted runoff depth and an MRE of up to  $-35.7\%$ . Future research should focus on developing a  $\lambda$  value optimization method and improve the prediction accuracy of short-duration and high-intensity rainstorm events.

## Conclusions

To optimize the soil conservation service curve number (SCS-CN) model to better predict runoff events in the mountainous region of Beijing, our study demonstrated that substantial prediction errors occur if the variation of the runoff curve number of individual runoff events is not taken into account (i.e., if only an averaged value is implemented). Our study accounted for the effect of rainfall processes and characteristics on surface runoff by proposing an SCS-CN calculation method for each runoff event ( $CN_t$ ). Moreover, the proposed method achieved satisfactory prediction accuracy. Therefore, our findings could provide technical support for the evaluation of water and soil resources and water conservation in this area.

1. When implementing the SCS-CN model to simulate runoff in the mountainous area of Beijing, a large simulation deviation may be observed if the variation of the runoff curve number of individual runoff events is not taken into account (i.e., if only an averaged value is implemented). To improve the SCS-CN model, the effect of rainfall on surface runoff was considered, and the  $P_X/P$  ratio (i.e., the ratio between the maximum  $X$ -minute rainfall ( $P_X$ ) and the total rainfall amount for each rainfall event ( $P$ )) was used to reflect the degree of temporal rainfall distribution. There was a significant positive correlation between the  $CN_t/CN_1$  and  $P_X/P$  ratios. Therefore, our study proposed a power function equation to calculate  $CN_t$  and provided the  $CN_1$ ,  $a$ , and  $b$  values for said equation under different land use types.
2. The efficiency coefficient ( $E_f$ ), correlation coefficient ( $r$ ), and mean relative error (MRE) of the Nash model were used to compare the predicted runoff depth with the observed runoff depth to assess the simulation performance of the optimized SCS-CN model at different  $X$  and  $\lambda$  values. The model simulation was optimal ( $E_f=0.791$ ;  $r=0.895$ ;  $MRE=-5.09\%$ ) when  $X=5$  min and  $\lambda=0.01$ , whereas the non-optimized SCS-CN model exhibited an  $E_f$  value below 0.05, demonstrating that the simulation accuracy of the optimized model was significant. When predicting surface runoff in the mountainous areas of Beijing, large prediction errors are likely to be observed if rainfall characteristics and the effects of high-intensity rainfall are not taken into account.
3. The optimized model had a satisfactory simulation performance for runoff events in average and wet conditions ( $E_f=0.883$ ;  $r=0.942$ ;  $MRE=0.56\%$ ). In both cases, the soil moisture content was relatively higher and was close to or equal to the field water holding during the production and flow processes. The optimized model had a relatively good simulation performance for runoff generation in bare land and cultivated land ( $E_f=0.831$ ;  $r=0.922$ ;  $MRE=13.67\%$ ). Moreover, the simulation performance for grassland exhibited  $E_f$ ,  $r$ , and MRE values of 0.603, 0.852, and 15.26%; however, the model was found to be unsuitable for runoff simulation in arboreal sand shrub land. The production and flow mechanisms in arboreal land are more complex and may arise from over-infiltration and over-holding processes under certain rainfall conditions. After optimization, the model exhibited a satisfactory simulation performance for production and flow events with rainfall duration  $t \geq 2$  h; however, the initial loss prediction was overestimated for runoff events with  $t < 2$  h, resulting in low predicted runoff depth. Therefore, future research should aim to develop a  $\lambda$  value optimization method and improve the prediction accuracy of runoff resulting from short-duration and high-intensity rainstorms.
4. Soil surface moisture during and after the rainfall can reflect the surface soil water content attributable to rainfall, and there is a significant power function decreasing relationship between said parameters and  $CN_t/CN_1$ . Under constant rainfall conditions, surface runoff decreases as water is replenished into the soil, which is reflected by a decrease in  $CN_t$ .

**Funding** This work was financially supported by the Natural Science Foundation of China (41401560, 51609259), by the National Key research and develop Program of China (2018YFC1508702, 2016YFC0400106-2), and by the Research

Program of China Institute of Water Resources and Hydropower Research (JZ0145B472016, JZ0145B862017).

### Compliance with ethical standards

**Conflict of interest** The authors declare that they have no conflict of interest.

### References

- Ajmal, M., Waseem, M., Ahn, J. H., & Kim, T. W. (2016). Runoff estimation using the NRCS slope-adjusted curve number in mountainous watersheds. *Journal of Irrigation and Drainage Engineering*, *142*(4), 04016002,1–04016002,0401600212.
- Boughton, W. C. (1989). A review of the USDA SCS curve number method. *Australian Journal of Soil Research*, *27*(3), 511–523.
- Chen, Z. W., Liu, X. N., & Zhu, B. (2014). Runoff estimation in hillslope cropland of purple soil based on SCS-CN model. *Transactions of the Chinese Society of Agricultural Engineering*, *30*(7), 72–81 (in Chinese with English abstract).
- Choi, D., Park, H., Kim, Y. J., Jung, J. W., Choi, W. J., Her, Y. J., et al. (2019). Curve numbers for rice paddies with different water management practices in Korea. *Journal of Irrigation and Drainage Engineering*, *145*(5), 06019003. [https://doi.org/10.1061/\(ASCE\)IR.1943-4774.0001382](https://doi.org/10.1061/(ASCE)IR.1943-4774.0001382).
- Deshmukh, D. S., Chaube, U. C., Hailu, A. E., Gudeta, D. A., & Kassa, M. T. (2013). Estimation and comparison of curve numbers based on dynamic land use land cover change, observed rainfall-runoff data and land slope. *Journal of Hydrology*, *492*, 89–101.
- Fadadu, M. H., Shrivastava, P. K., & Dwivedi, D. K. (2018). Application of Horton's infiltration model for the soil of Dediapada (Gujarat), India. *Journal of Applied & Natural Science*, *10*(4), 1254–1258.
- Fu, S. H., Zhang, G. H., Wang, N., & Luo, L. F. (2011). Initial abstraction ratio in the SCS-CN method in the Loess Plateau of China. *Transactions of the ASABE*, *54*(1), 163–169.
- Fu, S. H., Wang, H. Y., Wang, X. L., Yuan, A. P., & Lu, B. J. (2013). The runoff curve number of SCS-CN method in Beijing. *Geographical Research*, *32*(5), 797–807 (in Chinese with English abstract).
- Hosseini, S. M., & Mahjouri, N. (2018). Sensitivity and fuzzy uncertainty analyses in the determination of SCS-CN parameters from rainfall-runoff data. *Hydrological Sciences Journal*, *63*(3), 457–473.
- Huang, M. B., Gallichand, J., Wang, Z. L., & Goulet, M. (2006). A modification to the soil conservation service curve number method for steep slopes in the Loess Plateau of China. *Hydrological Processes*, *20*(3), 579–589.
- Huang, M. B., Gallichand, J., Dong, C. Y., Wang, Z. L., & Shao, M. A. (2007). Use of soil moisture data and curve number method for estimating runoff in the Loess Plateau of China. *Hydrological Processes*, *21*(11), 1471–1481.
- Jiao, J., Du, P. F., & Lang, C. (2015). Nutrients concentrations and fluxes in the upper catchment of the Miyun reservoir, China, and potential nutrient reduction strategies. *Environmental Monitoring and Assessment*, *187*(3), 110–124.
- Lal, M., Mishra, S. K., Ashish, P., Pandey, R. P., Meena, P. K., Chaudhary, A., et al. (2017). Evaluation of the Soil Conservation Service curve number methodology using data from agricultural plots. *Hydrogeology Journal*, *25*, 151–167.
- Lal, M., Mishra, S. K., & Kumar, M. (2019). Reverification of antecedent moisture condition dependent runoff curve number formulae using experimental data of Indian watersheds. *Catena*, *173*, 48–58.
- Li, X. S., Wu, B. F., & Zhang, L. (2013). Dynamic monitoring of soil erosion for upper streams of Miyun reservoir in the last 30 years. *Journal of Mountain Science*, *10*(5), 801–811.
- Li, J., Liu, C. M., Wang, Z. G., & Liang, K. (2015). Two universal runoff yield models: SCS vs. LCM. *Journal of Geographical Science*, *25*(3), 311–318.
- Luo, L. F., Zhang, K. L., & Fu, S. H. (2002). Application of runoff curve number method on Loess Plateau. *Bulletin of Soil and Water Conservation*, *22*(3), 58–61, 68 (in Chinese with English abstract).
- Mu, H. Q. (1992). Application of SCS procedure in Shiqiaoyu watershed[J]. *Journal of Hydraulic Engineering*, *10*(79–83), 89 (in Chinese with English abstract).
- Nash, J. E., & Sutcliffe, J. V. (1970). River flow forecasting through conceptual models part I: a discussion of principles. *Journal of Hydrology*, *10*(3), 282–290.
- Natural Resources Conservation Service. (2009). National Engineering Handbook, section 4: Hydrology, version. In *National Engineering Handbook. Engineering Division*. Washington, D C: US Department of Agriculture.
- Nigam, G. K., Sahu, R. K., Sinha, M. K., Deng, X., Singh, R. B., & Kumar, P. (2017). Field assessment of surface runoff, sediment yield and soil erosion in the opencast mines in Chirimiri area, Chhattisgarh, India[J]. *Physics and Chemistry of the Earth*, *101*, 137–148.
- Sharpley, A. N., & Williams, J. R. (1990). *EPIC-Erosion/Productivity Impact Calculator: 1. Model Documentation*. US Department of Agriculture Technical Bulletin No. 1768. Washington, DC: US Government Printing Office.
- Shi, Z. H., Chen, L. D., Fang, N. F., Qin, D. F., & Cai, C. F. (2009). Research on the SCS-CN initial abstraction ratio using rainfall-runoff event analysis in the Three Gorges Area, China. *Catena*, *77*(1), 1–7.
- U S Department of Agriculture-Soil Conservation Service. (1972). *SCS National Engineering Handbook, section 4: hydrology*. Washington D C: U S Department of Agriculture.
- Viji, R., Prasanna, P. R., & Ilangoan, R. (2015). Modified SCS-CN and green-ampt methods in surface runoff modelling for the Kundahpallam watershed, Nilgiris, Western Ghats, India. *Aquatic Procedia*, *4*, 677–684.
- Wang, T., Xu, H. L., & Bao, W. M. (2016). Application of isotopic information for estimating parameters in Philip infiltration model. *Water Science and Engineering*, *9*(4), 287–292.
- Wei, W. Q., & Xie, S. Q. (1992). The application of remote sensing in runoff formation in SCS model. *Remote Sensing of environment China*, *7*(4), 243–250 (in Chinese with English abstract).

- Wilken, F., Baur, M., Sommer, M., & Deumlich, D. (2018). Uncertainties in rainfall kinetic energy-intensity relations for soil erosion modelling. *Catena*, 171, 234–244.
- Wilson, L. E., Ramirez-Avila, J. J., & Hawkins, R. H. (2017). Runoff curve number estimation for agricultural systems in the southern region of USA. *World Environmental and Water Resources Congress*, 353–366.
- Wischmeier, W. H., & Smith, D. D. (1978). *Predicting rainfall erosion losses: a guide to conservation planning//Agriculture Handbook. No.537*. Washington D C: U S Department of Agriculture.
- Wu, X. L., Wei, Y. J., Wang, J. G., Xia, J. W., Cai, C. F., & Wei, Z. Y. (2018). Effects of soil type and rainfall intensity on sheet erosion processes and sediment characteristics along the climatic gradient in central-south China. *Science of the Total Environment*, 621, 54–66.
- Xiao, B., Wang, Q. H., Fan, J., Han, F. P., & Dai, Q. H. (2011). Application of the SCS-CN model to runoff estimation in a small watershed with high spatial heterogeneity. *Pedosphere*, 21(6), 738–749.

**Publisher's note** Springer Nature remains neutral with regard to jurisdictional claims in published maps and institutional affiliations.